Geomicrobiology Journal, 26:93–103, 2009

ISSN: 0149-0451 print / 1521-0529 online
DOI: 10.1080/01490450802660573

Taylor & Francis
Taylor & Francis Group

Formation of Cell-Iron-Mineral Aggregates by Phototrophic and Nitrate-Reducing Anaerobic Fe(II)-Oxidizing Bacteria

S. Schädler,[1] C. Burkhardt,[2] F. Hegler,[1] K.L. Straub,[1] J. Miot,[3] K. Benzerara,[3] and A. Kappler[1]

[1]*Geomicrobiology Group, Center for Applied Geosciences, University of Tuebingen, Germany*
[2]*Natural and Medical Sciences Institute (NMI) at the University of Tuebingen, Germany*
[3]*Institut de Minéralogie et de Physique des Milieux Condensés, UMR 7590, CNRS, Universités Paris 6 et Paris 7, France*

Microbial anaerobic Fe(II) oxidation at neutral pH produces poorly soluble Fe(III) which is expected to bind to cell surfaces causing cell encrustation and potentially impeding cell metabolism. The challenge for Fe(II)-oxidizing prokaryotes therefore is to avoid encrustation with Fe(III). Using different microscopic techniques we tracked Fe(III) minerals at the cell surface and within cells of phylogenetically distinct phototrophic and nitrate-reducing Fe(II)-oxidizing bacteria. While some strains successfully prevented encrustation others precipitated Fe(III) minerals at the cell surface and in the periplasm. Our results indicate differences in the cellular mechanisms of Fe(II) oxidation, transport of Fe(II)/Fe(III) ions, and Fe(III) mineral precipitation.

Keywords Fe(II) oxidation, iron-cycling, geomicrobiology

INTRODUCTION

Some prokaryotes have the ability to utilize iron as electron donor or electron acceptor for energy conservation in enzymatically catalyzed redox reactions (Ghiorse 1984; Kappler and Straub 2005; Weber et al. 2006; Ehrlich and Newman 2008). Iron redox transformation significantly affects many other biogeochemical cycles (e.g. carbon, phosphorous, sulfur) and influences the mobilization, immobilization and transformation of organic and inorganic pollutants (Stumm and Sulzberger 1992; Thamdrup 2000; Cornell and Schwertmann 2003; Neubauer et al. 2007).

The oxidation of Fe(II) by molecular oxygen is very slow at acidic pH but it can be catalyzed effectively by acidophilic microorganisms (Blake et al. 1992). At neutral pH, Fe(II) is oxidized by O_2 within minutes (Stumm and Morgan 1995) and neutrophilic aerobic Fe(II)-oxidizers have to compete with this abiotic reaction (Emerson and Moyer 1997). In anoxic environments, Fe(II) is relatively stable since neither nitrate nor sulfate react chemically with Fe(II) at appreciable rates at low temperature and only Mn(IV) and high concentrations of nitrite have been shown to be relevant chemical oxidants for Fe(II) (Buresh and Moraghan 1976; Rakshit et al. 2008). Therefore, anaerobic Fe(II)-oxidizing microbes represent the most important catalysts for Fe(II) oxidation under anoxic conditions (Kappler and Straub 2005).

Microorganisms catalyze the oxidation of Fe(II) under pH-neutral anoxic conditions either with light as energy source (Widdel et al. 1993) or with nitrate as electron acceptor (Straub et al. 1996) according to the following equations:

$$\text{Photosynthetic Fe(II) oxidation} : 4Fe^{2+} + CO_2 + 11\ H_2O + h\nu \rightarrow CH_2O + 4\ Fe(OH)_3 + 8H^+$$

$$\text{Nitrate-dependent Fe(II) oxidation} : 10Fe^{2+} + 2NO_3^- + 24H_2O \rightarrow 10Fe(OH)_3 + N_2 + 18H^+$$

where <CH_2O> is an approximate formula of biomass.

At circumneutral pH, both aerobic and anaerobic iron oxidizers face the problem of very poor solubility of one end product of their metabolism, i.e., Fe(III), with concentrations of dissolved Fe(III) in the nM to μM range (Stumm and Morgan 1995). At neutral pH, ferric iron (hydr)oxides are expected to precipitate more or less instantly as Fe(III) is formed due to its low solubility under these conditions. This precipitation depends on the geochemical conditions and Fe(III) concentrations and in many cases it occurs even directly where the Fe(III) is formed (i.e., likely on a membrane). Furthermore, the formed particles are positively charged due to their high points of net zero charge (ZPC): e.g., pH ~7.9 for ferrihydrite, pH 9.0–9.4 for goethite (Schwertmann and Cornell 2000) (7.5–9.5 depending on the literature), and pH 8.5 for hematite (Jeon et al. 2004). If present in the proximity of cells, Fe(III) ions, Fe(III) colloids and Fe(III) minerals would therefore be expected to adsorb to prokaryotic cell surfaces that are in general negatively charged due to a high content of carboxylic, phosphoryl and/or hydroxyl groups. Formation of mineral crusts would potentially limit the diffusion of substrates and nutrients to the cell, impair uptake of these compounds across the membrane, and as a consequence lead to the stagnation of cell metabolism and eventually to cell death.

For stalk- or sheath-forming aerobic Fe(II)-oxidizing bacteria of the genera *Gallionella* and *Leptothrix* it was suggested that microbially produced and excreted organic matrices are used for extra-cellular capture of Fe(III) minerals produced during aerobic Fe(II) oxidation (Hanert 1981; Emerson and Revsbech 1994). It has to be kept in mind that Fe(II) oxidation by *Leptothrix* is not associated with energy production and the site of Fe(II) oxidation therefore may be determined not by the need to produce maximum energy, but rather by the need to deposit Fe(III) in a particular location (i.e., sheath) or by the properties of the sheath itself. Nevertheless, the following questions remain unanswered: i) where the Fe(II) is oxidized (in the cytoplasm, in the periplasm or at the cell surface) and, ii) in the case of intracellular oxidation, how the Fe(III) is transported from the cytoplasm to the cell surface and the organic templates.

Even less is known about the mechanisms of Fe(II) oxidation in neutrophilic anaerobic Fe(II)-oxidizing bacteria. In particular it is unknown how those species avoid encrustation of the cell surface with the Fe(III) minerals that they produce. It was suggested that phototrophic Fe(II)-oxidizing bacteria oxidize Fe(II) at the cell surface (Kappler and Newman 2004), posing questions of how the electrons are then transported from the outside to the inside of the cell and why the positively charged Fe(III) does not bind to the negatively charged cell surface. Recently it was proposed that Fe(II) oxidation by the photoautotrophic strains "*Rhodobacter ferrooxidans*" strain SW2 and *Rhodopseudomonas palustris* strain TIE-1, happens in the periplasm of the cells (Croal et al. 2004; Jiao et al. 2007). Since cell encrustation was observed for neither of the strains (Kappler and Newman 2004; Jiao et al. 2005), this raises the question how Fe(III) is transported to the cell exterior and then away from the cells following periplasmic Fe(II) oxidation. The possibility of a pH microenvironment was suggested for strain SW2 (Kappler and Newman 2004) and neutrophilic aerobic Fe(II)-oxidizers (Sobolev and Roden 2001). A lower pH would potentially keep the Fe(III) in solution in close cell proximity and lead to controlled Fe(III) mineral precipitation at a certain distance from the cell surface. Alternatively, the use of organic ligands as complexing and solubilization agents has been suggested (Croal et al. 2004), although no evidence for such molecules has yet been found. In summary, presently it is not known where Fe(II) oxidation takes place in neutrophilic Fe(II) oxidizers (at the surface of the outer membrane, in the periplasm or even in the cytoplasm).

In order to identify the Fe(II) oxidation and Fe-transport mechanisms of neutrophilic anaerobic Fe(II)-oxidizing bacteria, it is necessary to evaluate whether various Fe(II)-oxidizing strains show differences in the localization of Fe(II) oxidation sites, in transport of Fe(II) and Fe(III) ions, and in Fe(III) mineral precipitation. In this study, we characterized cell-mineral aggregates formed by phototrophic and nitrate-reducing anaerobic Fe(II)-oxidizing bacteria using different microscopic techniques. In particular, the objective of this work was to determine the spatial allocation of Fe(III) minerals relative to the cells that produced these minerals.

METHODS AND MATERIALS

Bacterial Cultures

The following anoxygenic phototrophic Fe(II)-oxidizing cultures from our own culture collection including representatives from the phylum Proteobacteria and from the phylum Chlorobi were used: the purple sulfur bacterium (PSB) *Thiodictyon sp.* strain F4, a highly enriched culture (Croal et al. 2004), the green sulfur bacterium (GSB) *Chlorobium ferrooxidans* sp. strain KoFox, growing in a defined coculture with *Geospirillum* Ko Fum sp. (Heising et al. 1999), and the purple non-sulfur bacterium (PNSB) "*Rhodobacter ferrooxidans*" strain SW2 (Ehrenreich and Widdel 1994). In addition to these phototrophic strains, we chose a lithotrophic nitrate-reducing Fe(II)-oxidizing enrichment culture (Straub et al. 1996) and *Acidovorax* sp. strain BoFeN1, a mixotrophic nitrate-reducing Fe(II)-oxidizing strain (Kappler et al. 2005) for our experiments. By this selection we cover both nitrate-reducing and phototrophic Fe(II)-oxidizing bacteria including autotrophic and mixotrophic strains from different phylogenetic groups.

Growth Medium and Cultivation Conditions

Bacteria were cultivated in freshwater mineral medium with Fe(II), hydrogen, or acetate as electron donor at pH 6.8–7.0, as described previously (Straub et al. 1996; Kappler and Newman 2004; Hegler et al. 2008). Phototrophic Fe(II)-oxidizing cultures were incubated at 20°C and light saturation (>700 lux). Nitrate-reducing Fe(II)-oxidizing bacteria were incubated at 28°C in the dark. Fe(II) oxidation was followed by quantification of remaining Fe(II) in the cultures by a spectrophotometric test with ferrozine as described previously (Kappler and Newman 2004).

Received 17 September 2008; accepted 29 October 2008.
Present affiliation for K. L. Straub is Department of Environmental Geosciences, University of Vienna, Austria. This work was supported by an Emmy-Noether fellowship and several research grants from the German Research Foundation (DFG) to Andreas Kappler and a BMBF research grant (13N8652) to the Natural and Medical Sciences Institute at the University of Tuebingen. Some of the TEM images were taken by R. Mielke during a DFG-funded postdoctoral fellowship of AK in the laboratory of Prof. Dianne Newman at the California Institute of Technology. We would like to thank N.R. Posth and P. Larese-Casanova for their helpful comments in improving the manuscript. We thank Stephan Borensztajn from Laboratoire Interfaces et Systemes electrochimiques, UPR 15 CNRS, for SEM imaging. KB and JM are also grateful to Region Ile-de-France for the SESAME 2000 E1435 grant for the acquisition of the JEOL 2100F TEM at IMPMC UMR 7590.
Address correspondenc to Andreas Kappler, Geomicrobiology Group, Center for Applied Geosciences, University of Tübingen, Sigwartstrasse 10, D-72076 Tübingen, Germany. E-mail: andreas.kappler@uni-tuebingen.de

Downloaded By: [Kappler, Andreas] At: 19:47 20 February 2009

Sampling and Sample Preparation for Light and Electron Microscopy

Samples were taken at the late exponential growth phase when Fe(II) was almost completely oxidized. For light and scanning electron microscopy (SEM), 1 ml of a culture was taken with sterile syringes that had been flushed with N_2/CO_2. Light microscopy images of the samples were taken with a Zeiss AxioVison microscope equipped with an oil immersion object lens. For SEM, samples were chemically fixed using a half-strength Karnovsky solution (Kiernan 2000), placed on holey carbon-coated EM-copper-grids, dehydrated in subsequent steps with an increasing concentration of isopropanol, and finally dried in the Critical Point Dryer Bal-Tec CPD030, as previously described (Schaedler et al. 2008). Dried samples were mounted on aluminum stubs using double-sided carbon tape. For enhanced electrical conductivity, the edges of the EM grids were painted with conductive silver paste. Samples that showed strong surface charging were coated in a Balzers sputter coater SCD 40 (Bal-Tec, Balzers, Liechtenstein) with a thin layer of Au/Pd (90%/10% w/w). The coating thickness was approximately 20 nm (determined in focused ion beam cross-sections and by a surface texture analyzer; results not shown).

For transmission electron microscopy (TEM), cells were fixed for at least 2 hours in 1 to 3% (v/v) glutaraldehyde at 4°C, centrifuged for a few minutes at 6500 rpm and subsequently washed 3 times in distilled water or sodium cacodylate buffer (pH 7.2).

Electron Microscopy Techniques

Scanning Electron Microscopy. Imaging was performed with a Zeiss Gemini 1550VP FE-SEM, a Zeiss Gemini 1540XB FIB/FE-SEM, and a Zeiss Ultra 55, SEM-FEG microscope. A dual-beam focused ion beam (FIB) mounted on a Zeiss Gemini 1540XB was used for simultaneous milling and imaging at a working distance (SEM) of approx. 5 mm. Both microscopes were equipped with Everhart-Thornley SE detectors and in-lens detectors and were optimized to a lens aperture of 30 μm. Images were recorded in a format of 1024 × 768 pixels, at integration times between 15 μs and 45 μs per pixel.

Transmission Electron Microscopy and Scanning Transmission Electron Microscopy. For transmission electron microscopy, one half of each sample was stained in either 1% or 2% osmium tetroxide for at least 90 min and rinsed 3 times in distilled water. Stained and unstained samples were then dehydrated in increasing concentrations of either acetone or graded ethanol and propylene oxide-1,2 and embedded in epoxy resin. After 24 h at 60°C, samples were cut on a MT-X Ultramicrotome or a LEICA ultramicrotome (EM-UC6) with a 55° Diatome diamond knife to a 60 or 70 nm thickness. Ultrathin sections were placed on 200 mesh copper grids.

The prestained samples were subsequently poststained with 2% uranyl acetate for 5 min and lead citrate (2 g·L^{-1}) for 7 min before final imaging. An Akashi EM-002B microscope operating at 100 kV was used for microscopy and energy-dispersive X-ray spectroscopy EDS. The area sampled by the Oxford spectrum analyzer is approximately 8.8 nm at 83 kV. Acquisition rates were maintained at 10–20% dead time with 60 s live time. The electron beam was defocused at the condenser lens to maintain counting rates below 1 kHz and live time efficiency >95%. The EDS patterns were recorded on an INCA 3.04 Microanalysis Suite and digitized for analysis.

For scanning transmission electron microscopy (STEM), whole cells were deposited on a carbon-coated 200-mesh copper grid after two rinsing steps in degassed distilled water in an anoxic glove-box. STEM observations were performed with a JEOL2100 Microscope at IMPMC operating at 200kV in dark-field (DF) mode.

RESULTS

Association of Fe(II)-Oxidizing Cells with Fe(III) Minerals – Observations Using Light Microscopy

Light microscopy was performed in order to get a first overview of the spatial relation between cells and mineral phases in the cultures (Figure 1). This inspection showed clear differences between the arrangements of cells with respect to iron mineral precipitates for the different strains investigated in this study. Only cells of the mixotrophic nitrate-reducing Fe(II)-oxidizing strain BoFeN1 (Figure 1a) were mainly observed in association with iron precipitates. In cultures of all other Fe(II)-oxidizing strains – including the lithotrophic nitrate-reducing enrichment culture – most cells were not associated with iron precipitates (Figures 1 b, c, d).

Localization of Fe(III) Minerals – Visualization by Scanning Electron Microscopy

As compared to light microscopy, the higher resolution of scanning electron microscopy (SEM) allows a more detailed survey of cell surfaces and cell-mineral associations. Scanning electron micrographs of the mixotrophic anaerobic Fe(II)-oxidizing nitrate-reducing bacterium *Acidovorax* sp. strain BoFeN1, cultured in the presence of acetate and dissolved Fe(II), showed cell surfaces partly or entirely covered by globular iron mineral particles (Figures 2a, 2b). Cells that were covered to a different extent with iron globules of varying size (up to 150 nm) probably represented different growth stages of cells. Similarly shaped but smaller sized globular particles were described on coated SEM samples and attributed to sputter coating artefacts (Folk and Lynch 1997). Besides the different size of our structures compared to these sputtering artefacts, our observations of these particles were confirmed by transmission electron micrographs of uncoated samples, and neither the varying globule sizes nor the different extent of the encrustation can be explained by such artefacts.

In contrast, cells from the lithotrophic nitrate-reducing Fe(II)-oxidizing enrichment culture (Figures 3a, 3b) and cells

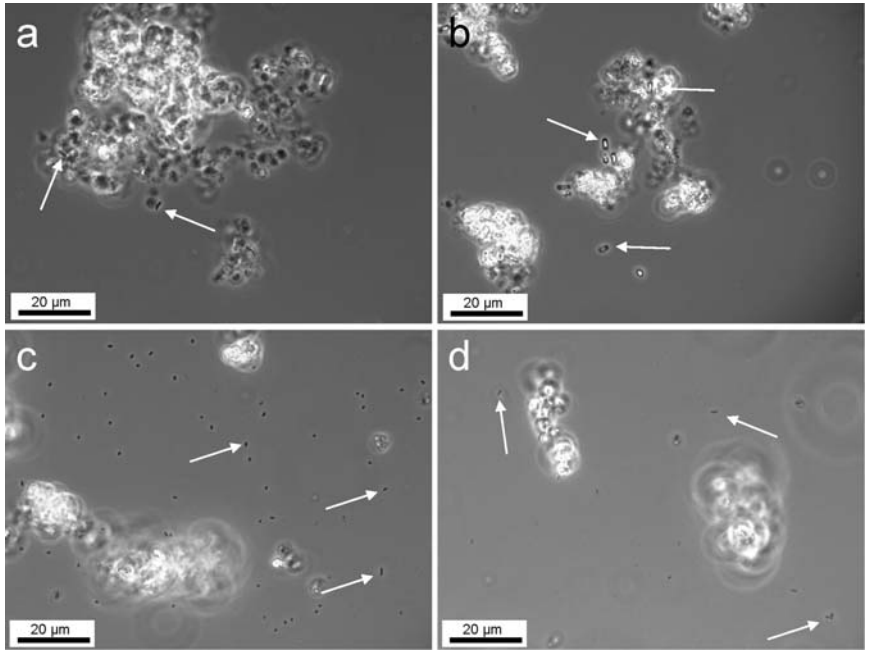

FIG. 1. Light microscopy images showing iron precipitates and cells (arrows) in cultures of *Acidovorax* sp. strain BoFeN1(a), *Thiodictyon* sp. strain F4 (b), *Chlorobium ferrooxidans* strain KoFox (c), and "*Rhodobacter ferrooxidans*" strain SW2 (d).

of the Fe(II)-oxidizing phototrophs *Chlorobium ferrooxidans* strain KoFox (Figures 3c, 3d) and *Thiodictyon* strain F4 (Figure 3e) to a large extent remained free of iron particles. The wrinkled cell surfaces of *Thiodictyon* strain F4 cells generally remained completely free of iron particles in all samples. Planktonic cells were observed, as were cells loosely associated with iron precipitates (Figure 3e). In cultures of *Rhodobacter* strain SW2, iron minerals were often observed along filamentous structures, which seemed to originate from the cell poles (Figure 3f). Sporadically SW2 cell surfaces were partially covered with iron particles (Figures 3g, 3h). When present at the surface of SW2 cells, the Fe(III) minerals seemed to develop at the cell poles first (Figures 3g, 3h).

In the coculture of *Chlorobium ferrooxidans* with *Geospirillum* sp. KoFum, we observed a significant difference: The surfaces of the Fe(II)-oxidizing *Chlorobium ferrooxidans* cells remained largely free of iron particles, with the exception of sparse, flat mineral particles that we will refer to as patches. In contrast, cell surfaces of *Geospirillum* sp. KoFum were observed to have a thin crust of globular particles with diameters in the order of several tens and up to one hundred nanometres (Figures 3c, 3d). Clearly, in this coculture only the Fe(II)-oxidizing strain was able to avoid encrustation.

Analysis of the Interior of Bulk Cell-Mineral Aggregates Using a Focused Ion Beam

Milling into bulk cell-mineral aggregates with a focused ion beam (FIB) creates cross-sections that allow for an insight into cell-mineral-aggregates. Bulky mineral structures from all phototrophic cultures and the lithotrophic nitrate-reducing enrichment culture were free of encrusted cells (data not shown). This indicates that none of the cells of these cultures became completely encrusted in iron minerals or deeply embedded in mineral structures. In contrast, the mixotrophic Fe(II)-oxidizing nitrate-reducing *Acidovorax* sp. strain BoFeN1 showed a range of slightly encrusted to heavily encrusted cells (Figures 2a, 2b). The images suggest that cell encrustation started by the formation of few small iron globules (Figure 2c), which grew during the course of Fe(II) oxidation (Figure 2d) and finally covered the complete cell surface (Figure 2e).

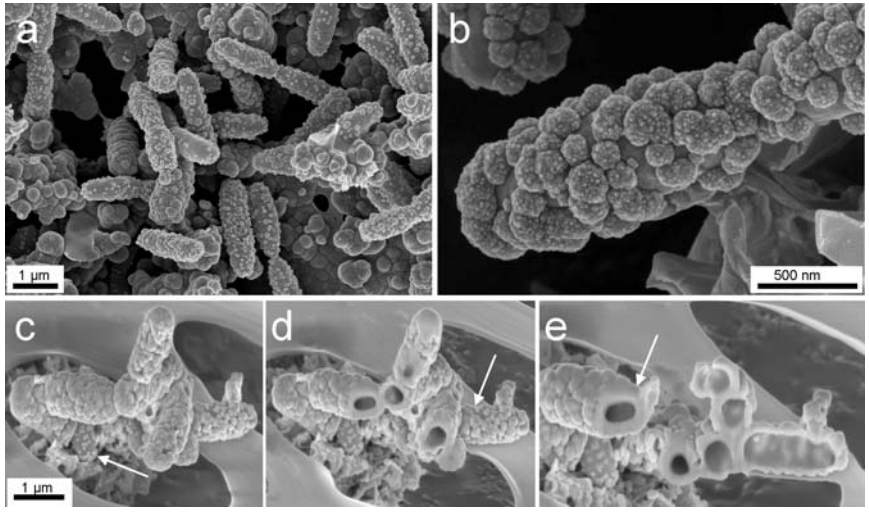

FIG. 2. Scanning electron micrographs of cells of the nitrate-reducing Fe(II)-oxidizing bacterium *Acidovorax* sp. strain BoFeN1 grown in the presence of Fe(II) (a–c). Images (d, e) show the same cells as (c) after milling with a focused ion beam (FIB). Different stages of encrustation can be observed from almost uncovered cells (c, arrow), partially covered cells (d, arrow), to completely covered cells (e, arrow). FIB milling current 10 pA, images taken using in-lens detectors, acceleration voltage 3 kV. Imaging quality in Figures (c-e) suffers from the ion milling process.

Observation of Cell Internal Structures by (Scanning) Transmission Electron Microscopy

Transmission electron microscopy (TEM) and scanning transmission electron microscopy (STEM) on ultramicrotomy sections revealed details from the cell interior as well as from the cell-mineral interface. We observed that *Acidovorax* sp. strain BoFeN1 cells contained iron minerals in the periplasm (Figures 4a–c, Figure 5). The thickness of the periplasmic mineral layer is approximately 30–40 nm (Figure 4a, Figure 5). The variations in thickness of the crust may be caused by the compression of samples during the preparation of thin sections; however, in particular the mineral layers at the pole regions appear to be thicker than along the cell body. The thicknesses of the two cell poles vary as well, which cannot be explained by preparation artefacts. Additionally, the presence of globular particles on the surface of the cells as previously observed in scanning electron microscopy was confirmed (Figure 4d, Figure 5).

In contrast, the periplasm of *Rhodobacter* sp. strain SW2 cells did not show any electron dense particles (Figures 4e-f), suggesting that the periplasm is free of mineral phases. The iron minerals present in cultures of *Rhodobacter* sp. strain SW2 have a fluffy and poorly crystalline appearance with μm sized primary particles that were rather loosely attached to or associated with the cell surfaces.

DISCUSSION

Neutrophilic Fe(II)-oxidizing bacteria face the problem of a poorly soluble metabolic end product, i.e., Fe(III). As a first step towards understanding the mechanisms of Fe(II) oxidation, Fe(III) transport, Fe(III) release, and iron mineralization, we investigated cell-mineral aggregates and localized Fe(III) minerals in the cells and at the cell surface. The responses of diverse strains of anerobic Fe(II)-oxidizing bacteria to the iron minerals they produce during growth were documented.

Cell-Mineral Aggregate Formation and Cell Encrustation

Our results give a first detailed overview of the spatial localization of iron oxides that were produced by 5 phylogenetically distinct cultures of anaerobic Fe(II)-oxidizing bacteria. The response of the cultures to ferric iron can be differentiated into non-encrustation and encrustation. Our study revealed non-encrusting Fe(II)-oxidizing cells in a lithotrophic nitrate-reducing enrichment culture and in phototrophic cultures of "*Rhodobacter ferrooxidans*" strain SW2, *Chlorobium ferrooxidans* strain KoFox, and *Thiodictyon sp*. strain F4. The surfaces of non-encrusting cells usually remained free of iron minerals with the minerals either loosely attached to the cells or localized at some distance. We observed cells encrusted with ferric iron

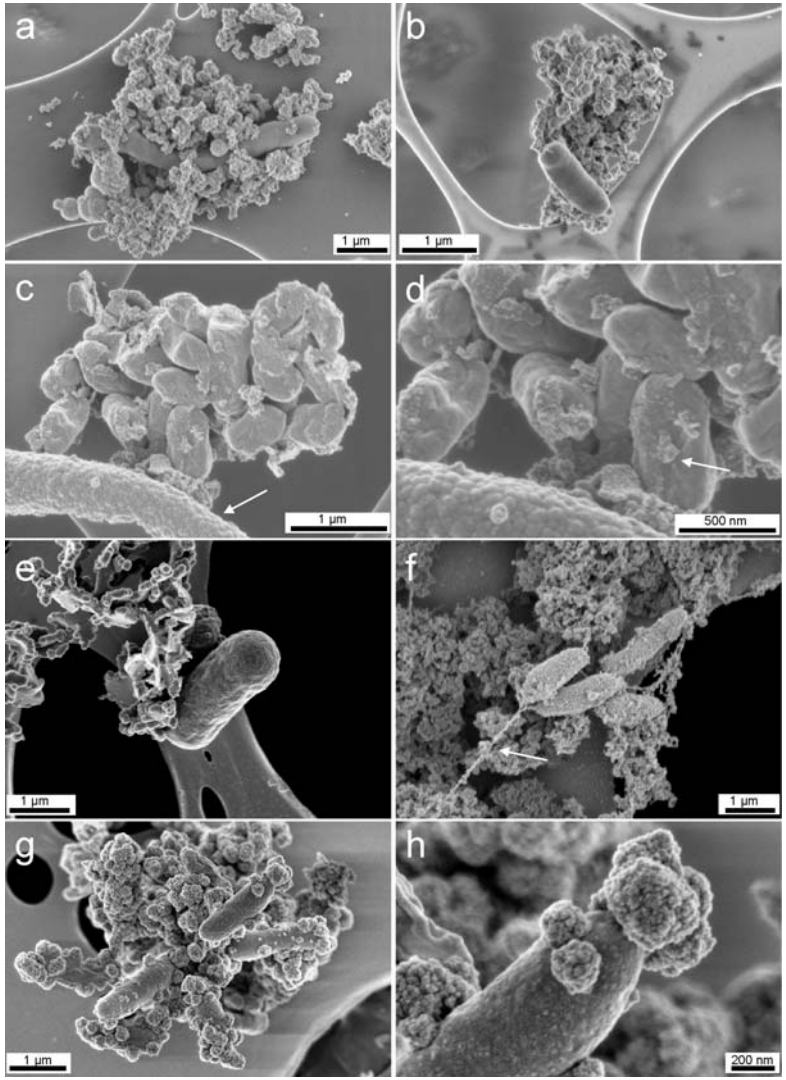

FIG. 3. Scanning electron micrographs of anaerobic Fe(II)-oxidizing cultures with non-encrusted, different-sized cells of the lithotrophic nitrate-reducing enrichment culture (a, b) and non-encrusted *Chlorobium ferrooxidans* strain KoFox cells with encrusted coculture strain *Geospirillum* sp. strain KoFum (arrow) (c, d). Fig. (d) is a close-up of (c) with focus on iron mineral patches on the cell surface of *Chlorobium ferrooxidans* (arrow). (e) Non-encrusted *Thiodictyon* sp. strain F4. (f) "*Rhodobacter ferrooxidans*" strain SW2 cells (non-encrusted) with filamentous structure (arrow) as well as the rare case of a partly mineral-covered cell surface (g, h). All images taken with in-lens detectors at acceleration voltages of 4 kV (a, b) 1 kV (c, d, f), or 2 kV (e, g, h).

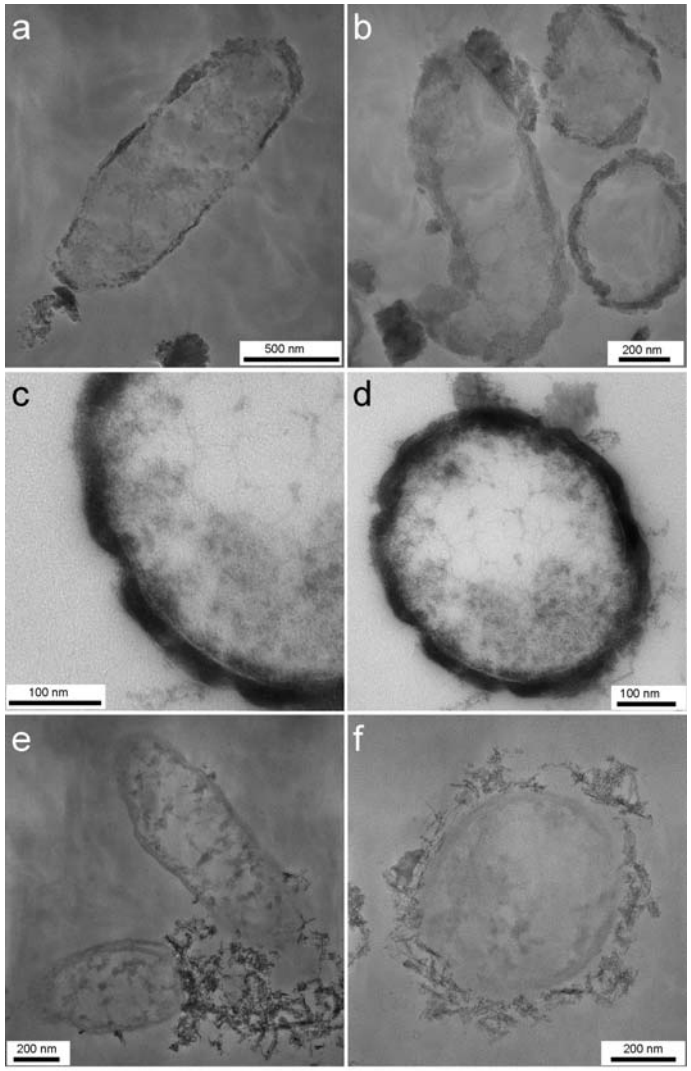

FIG. 4. Transmission electron micrographs of the nitrate-reducing Fe(II)-oxidizing bacterium Acidovorax sp. strain BoFeN1 grown in the presence of Fe(II) (a, b, c, d) showing encrustation of the cell surface and mineral precipitation in the periplasm. In contrast, cells of the phototrophic Fe(II)-oxidizing bacterium "*Rhodobacter ferrooxidans*" strain SW2 (e, f) show no encrustation, but a lose association with mineral particles. Stained samples.

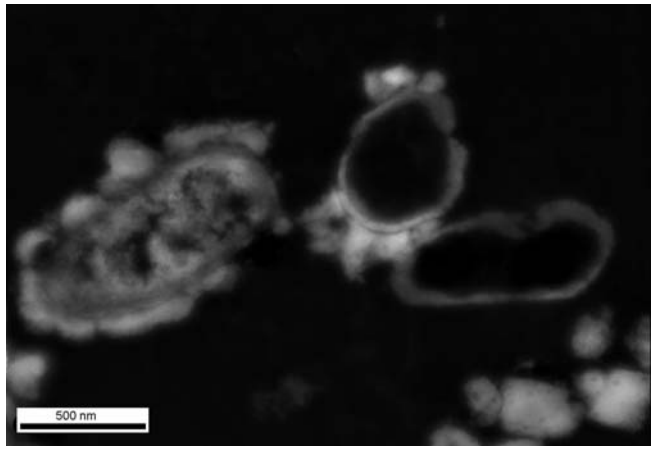

FIG. 5. Scanning transmission electron micrographs of cells of the nitrate-reducing Fe(II)-oxidizing bacterium *Acidovorax* sp. strain BoFeN1. Bright regions indicate the presence of Fe(III) in the periplasm and at the cell surface.

minerals only in the culture of the nitrate-reducing *Acidovorax* sp. strain BoFeN1.

Similarly, cells of the phototroph *Rhodomicrobium vannielii* strain BS-1 were described in an earlier study to encrust heavily with ferric iron minerals when the culture was grown in the presence of Fe(II) (Heising and Schink 1998). These contrasting observations suggest that fundamentally different Fe(II) oxidation and Fe(II)/Fe(III) transport mechanisms are present in non-encrusting and encrusting anaerobic Fe(II)-oxidizing bacteria. Furthermore, these differences cannot be related to a type of energy metabolism, i.e., respiration or photosynthesis.

The cell appendices observed in some samples of "*Rhodobacter ferrooxidans*" strain SW2 suggest that these cells excrete a fibrous extracellular material on which iron precipitates, possibly similar to *Gallionella* spp. cells that have been reported to produce extracellular organic fibers, forming twisted stalks and acting as a precipitation template for iron oxides (Emerson and Revsbech 1994; Hallberg and Ferris 2004).

Alternatively, it can be speculated that these extracellular fibres produced by strain SW2 could be involved in electron transfer to the cells in a similar way as described recently for the conductive pili in Fe(III)-reducing microorganisms (Gorby et al. 2005; Reguera et al. 2005): whereas the Fe-reducers putatively use the pili to transport electrons from the cells to the solid-phase electron acceptors (Fe(III) minerals), the Fe(II)-oxidizers could transport electrons from Fe(II) that sorbs to the organic structures to the cells. This would oxidize the Fe(II) to Fe(III) followed by Fe(III) mineral precipitation at the organic structures, thus preventing cell encrustation. Chan et al. (2004) suggested that the similar biologically produced filament structures that they observed, may serve as a precipitation template for mineralization of oxyhydroxides during microbial ferrous iron oxidation. These researchers also discussed the potential benefits of an increased pH gradient across the cell membrane (i.e., up to 4 H^+ per ferrous iron oxidized when goethite is formed), which may also be generated and harvested by SW2 cells.

In cocultures of the phototrophic Fe(II)-oxidizing *Chlorobium ferrooxidans* strain KoFox with *Geospirillum* sp. KoFum, only cells of strain KoFum were covered by iron minerals. Small patches of iron minerals at the surface of KoFox cells imply that these cells may produce extracellular precipitation templates (e.g., exopolysaccharides) at their cell surface–which they would need to shed after a certain time – and thus act similarly to the sheath-forming bacterium *Leptothrix ochracea* that uses an exopolysaccharide slime layer on which minerals are precipitated (Emerson and Revsbech 1994). Cells of strain KoFum were unable to oxidize ferrous iron (Heising et al. 1999). Hence, KoFum cells cannot encrust intracellularly, but the cell surfaces seemed to act as a passive template for iron biomineralization. The fact that the Fe(II)-oxidizing KoFox cells were not encrusted, but the co-culture KoFum cells were, potentially rules out a ligand-complexation-driven mechanism to avoid precipitation by the KoFox strain: In the presence of Fe(III)-solubilizing ligands encrustation would be expected for neither of the strains present in the culture, assuming similar cell-surface properties.

In cultures of the *Thiodictyon* sp. strain F4, the cells were free of minerals and no Fe(III) precipitation was observed on

the cells or on cell appendices. It is evident that these cells manage to precipitate Fe(III) minerals at a certain distance of the cell surface; although the way in which they do is presently unclear. A pH microenvironment keeping the Fe(III) in solution in close cell vicinity, in combination with exopolymers at which the Fe(III) then nucleates and precipitates, could be a potential mechanism (see later).

In contrast to these non-encrusting phototrophic Fe(II)-oxidizers, cells of the encrusting strain BoFeN1 appeared with iron-containing precipitates (possibly Fe(III) (hydr)oxides or Fe(III) phosphates) within the periplasm, as well as a cover of iron-containing globules on the surface. This appearance was similar to what was reported by Emerson and Moyer (1997) for the two neutrophilic Fe(II)-oxidizing strains ES-1 and ES-2. Similar precipitation within the periplasm has been previously observed for other microbial systems such as calcifying bacteria (e.g., Benzerara et al. 2004a, 2004b). However, the replacement of $FeCl_2$ by $CaCl_2$ in the culture medium of BoFeN1 did not lead to calcification (data not shown). These results suggest that the precipitation of Fe minerals in the periplasm is not due to preferential binding of positively charged ions (Ca^{2+} or Fe^{2+}) to the peptidoglycan or other biopolymers within the periplasm but rather due to oxidation of the Fe(II) with concomitant Fe(III) mineral precipitation.

In very few experiments, cells of SW2 cultures showed precipitation of Fe(III) minerals at the cell surface. It seemed that this mineral precipitation starts at the cell poles rather than the cell body. Likewise, the cell poles of BoFeN1 cells also often appeared more densely covered or more closely attached to Fe(III) precipitates and showed a thicker precipitate layer within the periplasm. Several hypotheses can be formulated, meriting further investigations: (1) The cell pole region is better accessible to diffusion of dissolved Fe(II) to and possibly into the cell; (2) It is plausible that the geometry of the spherical poles that yields to a lower surface/volume ratio as compared to the cylindrical cell body could possibly increase the surface charge density at the cell poles and may lead to preferential interaction with the positively charged Fe(III) phases (Shapiro et al. 2002). (3) Finally, it could be related to the older age of one of the poles in a bacterial cell and/or the concomitant higher accumulation of proteins within this pole that may play a role in periplasmic iron precipitation.

Mechanisms of Fe(II) Oxidation and Fe(III) Transport and Mineralization

Based on our observations, we suggest that different strains use different oxidation and iron transport mechanisms, which lead to the various interactions between iron minerals and the cells. Figure 6.1 shows different possibilities of how and where Fe(II) could be oxidized by the cells: dissolved Fe(II) diffuses to the cell surface where it can either be taken up into the periplasm (by diffusive uptake or a transport mechanism, Figure 6.1a) or bind to the cell surface (Figure 6.1b). In both cases it will be oxidized by an iron oxidase protein that is located either in the periplasm or at the cell surface respectively. A comparison to manganese-oxidizing bacteria shows that potential candidates for this protein are multi-copper oxidase (MCO)-like enzymes – suggested to be the mechanism of Mn(II) oxidation at bacterial surfaces by Tebo et al. (2004). A c-type cytochrome was suggested as another possibility to be the Fe(II) oxidoreductase in "*Rhodobacter ferrooxidans*" strain SW2 cells, most likely functioning in the cells' periplasm (Croal et al. 2007).

In the case of the Fe(II) oxidase being located in the periplasm, the poorly soluble Fe(III) produced can either leave the cell via an Fe(III) transport system and adsorb to the cell surface, or precipitate directly in the periplasm (Figure 6.1a). Strains which do not show encrustation obviously have a mechanism to maintain the Fe(III) produced during their metabolism in solution and to displace the position of precipitation of iron(hydr)oxides to a point distant from the cell's surface. Figure 6.2 sums up possible mechanisms. As suggested by Kappler and Newman (2004), organic ligands could form a dissolved Fe(III) complex, keeping the Fe(III) in solution, as depicted in Figure 6.2a. Alternatively, soluble colloidal Fe(III) species could be produced by the cells (Sobolev and Roden 2001).

A slightly acidic cell pH microenvironment (Figure 6.2b) was suggested to be generated by the proton motive force (PMF) (Urrutia et al. 1992). As a consequence of proton pumping, the pH in the cell wall of an actively metabolizing cell in a neutral bulk solution can decrease to pH values below 6 (Johnson et al. 2007). This would increase the solubility of Fe(III) and keep it in solution. As the Fe(III) diffuses away from the cell and thus towards a neutral pH where its solubility decreases, it meets a precipitation nucleus and forms a solid phase. Preventing cell-surface encrustation by diffusion of the positively charged Fe(III) away from the cell could be enhanced by a positively charged cell surface (Figure 6.2c). In these cases (presence of a pH micro-environment, a charged cell surface, or a combination of the two), exopolysaccharides could act as Fe(III) precipitation template (Chan et al. 2004). An exopolymer more negatively charged than the cell surface would be an explanation for precipitation distant to the cell.

Implications of Iron Biomineralization on Biosignature Formation

Several previous studies have looked for traces of Fe(II)-oxidizing bacteria in the geological record and in modern environments (e.g., Ghiorse 1984; Little et al. 2004; Ivarsson et al. 2008). However, the products and potential biosignatures left by bacteria with such a metabolism have until now been studied for only very few genera, such as *Gallionella* or *Leptothrix* (e.g., Hallberg and Ferris 2004; Fortin and Langley 2005). Consequently, our knowledge of the diversity of the biomineralization patterns that can potentially be observed is restricted. Although it is difficult here to presume what can be preserved after diagenesis and metamorphism, the present study offers

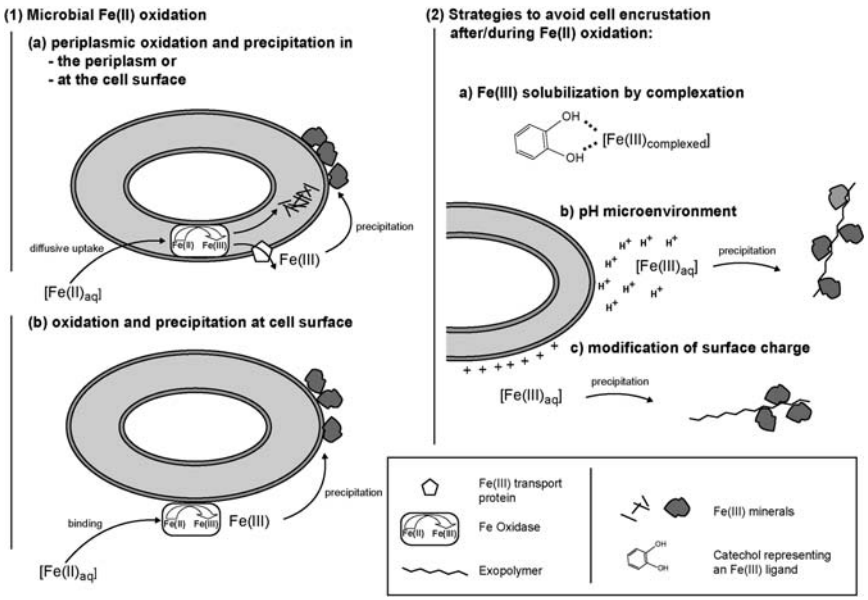

FIG. 6. Model for anaerobic Fe(II) oxidation (1) and suggested mechanisms that could avoid encrustation (2) by gram-negative cells.

some clues on the possible fossils that form during biomineralization by Fe(II)-oxidizing bacteria. It clearly shows that a significant diversity of biominerals exists, although all these strains grow in very similar culture media. Some bacteria can be fossilized as mineral shells corresponding to whole cells (e.g., BoFeN1) with preservation of their morphology and size due to the precipitation of minerals in their periplasm. SW2 cells can form small filamentous mineral structures that resemble pili.

Additional analyses are needed to see whether they are associated with organics similar to the structures observed by Chan et al. (2004) and may be preserved in the geological record. In contrast, some cells such as *Thiodictyon* sp. strain F4 do not leave any obvious specific signature in the mineral deposits suggesting the possibility of specific biases in the fossil record. Finally, it can be noted that in the case of KoFox and KoFum, interestingly, the one susceptible to leaving a fossil or a trace is not the one that oxidizes iron; therefore, looking for Fe(III)-precipitates associated with potential microfossils may be misleading. In any case, the combination of analyses of the mineralogy and texture of the iron precipitates with analyses of the organic molecules possibly preserved in the microfossils (e.g., Bernard et al. 2007) appears as a necessary approach to investigate the resulting microfossils.

Conclusions and Possible Further Experiments

Obviously different bacterial Fe(II)-oxidizing strains oxidize Fe(II) at different locations, i.e., at the cell surface or in the periplasm, and show different mechanisms of how to avoid encrustation with ferric iron. Suggested mechanisms are Fe(III) solubilization by complexation, creation of specific cellular pH microenvironments, modification of the cell surface charge, and production of cellular exopolymers that act as precipitation templates; any combination of these mechanisms is possible.

In order to evaluate the suggested mechanisms, further experiments are necessary to identify the Fe(II)-oxidizing mechanisms and enzymes as pioneered in the studies by Croal et al. (2007) and Jiao et al. (2007). Additionally, potential organic compounds (exopolysaccharides) acting as nucleation sites should be identified (e.g., by scanning transmission X-ray microscopy, STXM), the hypothesized cell pH microenvironment should be attempted to be visualized (e.g., by using a pH-dependent fluorophore), and the cell surface properties (cell surface charge) should be determined via titration.

REFERENCES

Benzerara K, Menguy N, Guyot F, Skouri F, de Lucca G, Heulin T. 2004a. Bacteria-controlled precipitation of calcium phosphate by *R. tataouinensis*. Earth Planet Sci Lett 228:439–449.

Benzerara K, Yoon TH, Tyliszczak T, Constantz B, Spormann AM, Brown GE. 2004b. Scanning transmission X-ray microscopy study of microbial calcification. Geobiology 2:249–259.

Bernard S, Benzerara K, Beyssac O, Menguy N, Guyot F, Brown GE, Goffé B. 2007. Exceptional preservation of fossil plant spores in high-pressure metamorphic rocks. Earth Planet Sci Lett 262(1–2):257–272.

Blake R, Shute EA, Waskovsky J, Harrison AP. 1992. Respiratory components in acidophilic bacteria that respire on iron. Geomicrobiol J 10(3–4):173–192.

Buresh RJ, Moraghan JT. 1976. Chemical reduction of nitrate by ferrous iron. J Environ Qual 5:320–325.

Canfield DE. 1989. Reactive iron in marine sediments. Geochim Cosmochim Acta 53:619–458.

Chan CS, De Stasio G, Welch SA, Girasole M, Frazer BH, Nesterova MV, Fakra S, Banfield JF. 2004. Microbial polysaccharides template assembly of nanocrystal fibers. Science 303:1656–1658.

Cornell RM, Schwertmann U. 2003. The iron oxides: structure, properties, reactions, occurrences and uses: Weinheim; Cambridge, VCH, xxxi, 573 p.

Croal LF, Johnson CM, Beard BL, Newman DK. 2004. Iron isotope fractionation by Fe(II)-oxidizing photoautotrophic bacteria. Geochim Cosmochim Acta 68(6):1227–1242.

Croal LF, Jiao Y, Newman DK. 2007. The fox operon from *Rhodobacter* strain SW2 promotes phototrophic Fe(II) oxidation in *Rhodobacter capsulatus* SB1003. J Bacteriol 189(5):1774–1782.

Ehrenreich A, Widdel F. 1994. Anaerobic oxidation of ferrous iron by purple bacteria, a new type of phototrophic mechanism. Appl Environ Microbiol 60(12):4517–4526.

Ehrlich HL, Newman DK. 2008. Geomicrobiology, Fifth Edition. Boca Raton, FL: CRC Press, 656p.

Emerson D, Moyer C. 1997. Isolation and characterization of novel iron-oxidizing bacteria that grow at circumneutral pH. Appl Environ Microbiol 63(12):4784–4792.

Emerson D, Revsbech NP. 1994. Investigation of an iron-oxidizing microbial mat community located near Aarhus, Denmark: Field studies. Appl Environ Microbiol 60(11):4022–4031.

Folk RL, Lynch FL. 1997. The possible role of nanobacteria (dwarf bacteria) in clay-mineral diagenesis and the importance of careful sample preparation in high-magnification SEM study. J Sediment Res 67(3):583–589.

Fortin D, Langley S. 2005. Formation and occurrence of biogenic iron-rich minerals. Earth Sci Rev 72:1–19.

Gerhardt S, Brune A, Schink B. 2005. Dynamics of redox changes of iron caused by light-dark variations in littoral sediment of a freshwater lake. Biogeochemistry 74:323–339.

Ghiorse WC. 1984. Biology of iron-depositing and manganese-depositing bacteria. Ann Rev Microbiol 38:515–550.

Gorby YA, Yanina S, McLean JS, Rosso KM, Moyles D, Dohnalkova A, Beveridge TJ, Chan IS, Kim BH, Kim KS, Culley DE, Reed SB, Romine MF, Saffarini A, Hill EA, Shi L, Elias DA, Kennedy DW, Pinchuk G, Watanabe K, Ishii S, Logan B, Nealson KH, Fredrickson JK. 2005. Electrically conductive bacterial nanowires produced by *Shewanella oneidensis* strain MR-1 and other microorganisms. Proc Natil Acad Sci 103(30):11359–11363.

Hallberg R, Ferris FG. 2004. Biomineralization by *Gallionella*. Geomicrobiol J 21:325–330.

Hanert HH. 1981. The genus *Gallionella*. In: The Prokaryotes.Starr MP, Stolp H, Trueper HG, Balows A, Schlegel HG (eds) Springer, Berlin, p. 509–515.

Hegler F, Posth NR, Jiang J, Kappler A. 2008. Physiology of phototrophic iron(II)-oxidizing bacteria – implications for modern and ancient environments. FEMS Microbiol Ecol. 66:250–260.

Heising S, Richter L, Ludwig W, Schink B. 1999. *Chlorobium ferrooxidans* sp. nov., a phototrophic green sulfur bacterium that oxidizes iron in coculture with a '*Geospirillum*' sp. strain. Arch Microbiol 172:116–124.

Heising S, Schink B. 1998. Phototrophic oxidation of ferrous iron by a *Rhodomicrobium vannielii* strain. Microbiology 144:2263–2269.

Ivarsson M, Lindblom S, Broman C, Holm NG. 2008. Fossilized microorganisms associated with zeolite-carbonate interfaces in sub-seafloor hydrothermal environments. Geobiology 6:155–170.

Jeon B, Dempsey BA, Burgos WD, Royer RA, Roden EE. 2004. Modeling the sorption kinetics of divalent metal ions to hematite. Water Res 38(10):2499–2504.

Jiao Y, Newman DK. 2007. The pio operon is essential for phototrophic Fe(II) oxidation in *Rhodopseudomonas palustris* TIE-1. J Bacteriol 189:1765–1773.

Jiao Y, Kappler A, Croal LR, Newman DK. 2005. Isolation and characterization of a genetically traceable photoautotrophic Fe(II)-oxidizing bacterium, *Rhodopseudomonas palustris* strain TIE-1. Appl Environ Microbiol 71:4487–4496.

Johnson KJ, Ams DA, Wedel AN, Szymanowski JES, Weber DL, Schneegurt MA, Fein JB. 2007. The impact of metabolic state on Cd adsorption onto bacterial cells. Geobiology 5:211–218.

Kappler A, Schink B, Newman DK. 2005. Fe(III) Mineral formation and cell encrustation by the nitrate-dependent Fe(II)-oxidizer strain BoFeN1. Geobiology 3:235–245.

Kappler A, Newman DK. 2004. Formation of Fe(III)-Minerals by Fe(II)-oxidizing photoautotrophic bacteria. Geochim Cosmochim Acta 68:1217–1226.

Kappler A, Straub KL. 2005. Geomicrobiological cycling of iron. Rev Mineral Geochem 59:85–108.

Kiernan JA. 2000. Formaldehyde, formalin, paraformaldehyde and glutaraldehyde: what they are and what they do. Microsc Today 1:8–12.

Little CTS, Glynn SEJ, Mills RA. 2004. Four-hundred-and-ninety-million-year record of bacteriogenic iron oxide precipitation at sea-floor hydrothermal vents. Geomicrobiol J 21:415–429.

Neubauer SC, Toledo-Durán GE, Emerson D, Megonigal JP. 2007. Returning to their roots: Iron-oxidizing bacteria enhance short-term plaque formation in the wetland-plant rhizosphere. Geomicrobiol J 24:65–73.

Rakshit S, Matocha CJ, Coyne MS. 2008. Nitrite reduction by siderite. Soil Sci Soc Amer J 72:1070–1077.

Reguera G, McCarthy KD, Mehta T, Nicoll JS, Tuominen MT, Lovley DR. 2005. Extracellular electron transfer via microbial nanowires. Nature 435:1098–1101.

Schaedler S, Burkhardt C, Kappler A. 2008. Evaluation of electron microscopic sample preparation methods and imaging techniques for characterization of cell-mineral aggregates. Geomicrobiol J 25:228–239.

Schwertmann U, Cornell RM. 2000. Iron Oxides in the Laboratory. Second edition. New York: Wiley.

Shapiro L, McAdams HH, Losick R. 2002. Generating and exploiting polarity in bacteria. Science 298:1942–1946.

Sobolev D, Roden EE. 2001. Suboxic deposition of ferric iron by bacteria in opposing gradients of Fe(II) and oxygen at circumneutral pH. Appl Environ Microbiol 67(3):1328–1334.

Straub KL, Benz M, Schink B, Widdel F. 1996. Anaerobic, nitrate-dependent microbial oxidation of ferrous iron. Appl Environ Microbiol 62:1458–1460.

Stumm W, Morgan JJ. 1995. Aquatic Chemistry: Chemical Equilibria and Rates in Natural Waters. New York: Wiley-Interscience. 1040 p.

Stumm W, Sulzberger B. 1992. The cycling of iron in natural environments: Considerations based on laboratory studies of heterogeneous redox processes. Geochim Cosmochim Acta 56:3233–3257.

Tebo BM, Bargar JR, Clement BG, Dick GJ, Murray KJ, Parker D, Verity R, Webb SM. 2004. Biogenic manganese oxides: Properties and mechanisms of formation. Ann Rev Earth Planet Sci 32:287–328.

Thamdrup B. 2000. Bacterial manganese and iron reduction in aquatic sediments. Adv Microb Ecol 16(16):41–84.

Urrutia MM, Kemper M, Doyle R, Beveridge TJ. 1992. The membrane-induced proton motive force influences the metal binding ability of *Bacillus subtilis* cell walls. Appl Environ Microbiol 58:3837–3844.

Weber KA, Achenbach LA, Coates JD. 2006. Microorganisms pumping iron: anaerobic microbial iron oxidation and reduction. Nature Rev Microbiol 4:752–764.

Widdel, F , Schnell S, Heising S, Ehrenreich A, Assmus B, Schink B. 1993. Ferrous iron oxidation by anoxygenic phototrophic bacteria. Nature 362:834–836.